Discover Oncology

ANALYSIS Open Access

Exploration of the roles of CAFs in melanoma based on single-cell transcriptomics and spatial transcriptomics

Sheng Hong[1†], Yuhan Zhao[2†], Anni Hu[3†], Yizhong Zhang[4†], Yuming Li[5], Yan Rong[5], Zukai Li[5], Wenzhuo Su[6*] and Lude Zhu[1*]

[†]Sheng Hong, Yuhan Zhao, Anni Hu and Yizhong Zhang have contributed equally to this work.

*Correspondence:
Wenzhuo Su
ahmuswz@163.com
Lude Zhu
zhulude0629@163.com

Full list of author information is available at the end of the article

Abstract

Background Cancer-associated fibroblasts (CAFs) are increasingly recognized as critical contributors to the limited efficacy of immunotherapy, particularly through the establishment of immune-excluded tumor microenvironments. However, the functional heterogeneity and spatial ecological roles of CAFs in melanoma remain poorly characterized.

Methods We integrated single-cell RNA sequencing, spatial transcriptomics, and bulk RNA-seq data to systematically dissect CAF molecular programs in melanoma using weighted gene co-expression network analysis (WGCNA). Spatial distribution, CellChat, and ligand–receptor interaction analyses were applied to construct CAF-centered immune exclusion networks. A functional scoring model (riskScore) based on the CAF-M1 module was developed to evaluate clinical relevance.

Results CAF was spatially co-localized with endothelial cells, and engaged in strong crosstalk with multiple immune cell types via pathways such as COLLAGEN–integrin and THBS1–CD47. The derived riskScore model demonstrated robust prognostic value across TCGA-SKCM cohort.

Conclusion Through spatial aggregation and multifaceted immune signaling, CAF constructs a multilayered immune-exclusion network in melanoma, linking stromal remodeling to immune evasion. These findings offer novel insights into CAF-driven immune resistance and may inform future stratified immunotherapeutic strategies.

Keywords Melanoma, CAFs, Single-cell RNA sequencing, Spatial transcriptomics

1 Introduction

Melanoma originates from pigment-producing melanocytes and is characterized by its aggressive invasiveness. It can rapidly penetrate the basal layer of the skin, enter the bloodstream and lymphatic system, and metastasize to distant organs such as the lungs, liver, brain, and bones, resulting in advanced-stage disease and poor prognosis [1]. In 2020, there were approximately 325,000 new melanoma cases and around 57,000 deaths

worldwide. By 2040, the number of new cases is projected to rise to about 510,000, with deaths reaching an estimated 96,000, indicating a notable upward trend [2].

In recent years, targeted therapies against key mutations such as BRAF and MEK, as well as immune checkpoint inhibitors (e.g., CTLA-4 and PD-1/PD-L1 antibodies), have significantly improved the prognosis of some patients with advanced melanoma, even enabling long-term remission in certain cases. However, treatment resistance, high relapse rates, and immune-related adverse events remain major challenges that limit overall clinical efficacy [3, 4]. One critical reason for the suboptimal response to immunotherapy is the widespread phenomenon of immune exclusion. Even when effector T cells are enriched around tumor tissue, they often fail to effectively infiltrate the tumor core due to physical barriers (e.g., dense stroma) or functional suppression (e.g., immunosuppressive factors and disrupted signaling), contributing to a so-called cold tumor microenvironment [5]. This process is typically driven by multiple immunosuppressive cell types, such as regulatory T cells, M2-type macrophages, and CAFs, along with their associated molecular mechanisms. Therefore, systematically identifying the key cellular components and regulatory pathways involved in immune suppression and T cell exclusion within the tumor microenvironment has become a central focus for improving immunotherapy response rates.

CAFs are key stromal components of the tumor microenvironment and are extensively involved in extracellular matrix (ECM) remodeling, angiogenesis, and immune regulation [6]. Recent studies have shown that CAFs play a critical role in promoting tumor immune exclusion, suppressing immune cell infiltration, and mediating resistance to immunotherapy [6]. CAFs can form physical barriers by secreting matrix components such as collagen, thereby restricting the migration of T cells into the tumor core; they can also release immunosuppressive factors such as TGF-β and CXCL12, which induce T cell exhaustion or promote the recruitment of regulatory immune cells, ultimately shaping an "immune-excluded" tumor microenvironment [7]. In skin cancers including melanoma, a study identified a conserved taxonomy comprising three CAF subsets: myofibroblastic (RGS5^{+}), matrix-producing (mCAF), and immunomodulatory (iCAF) populations. Crucially, their work demonstrated a dynamic repopulation of these subsets during tumor progression, with iCAFs becoming enriched in advanced disease [8].

Although the critical roles of CAFs have been increasingly recognized, CAFs themselves are highly heterogeneous, encompassing multiple functional states and molecular subtypes. Traditional studies have largely relied on single markers such as FAP and α-SMA (ACTA2) to define CAFs, which fails to fully capture their multidimensional functional characteristics [9]. In immune-dependent tumors such as melanoma, the specific roles of different CAF subpopulations in remodeling the immune microenvironment remain insufficiently characterized. For instance, CAFs located at the tumor periphery can secrete LOX protein to cross-link collagen, thereby enhancing the physical barrier and hindering T cell infiltration; meanwhile, inflammatory CAFs (iCAFs) within the tumor core secrete cytokines such as IL-6 to recruit immunosuppressive cells and foster an immunologically "cold" environment [7, 10]. Therefore, it is imperative to characterize the intrinsic heterogeneity of CAFs from a functional programming perspective and to identify key molecular modules involved in immune regulation, which will provide a foundation for further mechanistic studies and targeted interventions.

Against this background, the rapid advancement of single-cell sequencing technologies has provided unprecedented resolution for dissecting the heterogeneity and functional states of CAFs in melanoma. Compared with traditional subpopulation classifications based on marker genes, module-based strategies that identify gene co-expression patterns offer deeper insights into the potential functional programs and cooperative pathways of CAFs [11]. Meanwhile, the emergence of spatial transcriptomics has enabled the visualization and reconstruction of CAF localization within tumor tissues, their spatial relationships with immune cells, and their impact on the surrounding microenvironment [12]. Therefore, integrating single-cell and spatial multi-omics approaches to map the associations between CAF functional modules and tumor immune exclusion may offer novel perspectives on CAF-driven immune evasion mechanisms and uncover CAF-related molecular features with potential prognostic and therapeutic value.

In this study, using melanoma as a model, we integrated single-cell transcriptomics, spatial transcriptomics, and bulk RNA sequencing data to systematically investigate the functional programs of CAFs and their roles in immune exclusion. We first constructed a weighted gene co-expression network within CAFs and identified 16 distinct functional modules, focusing particularly on the CAF-M1 module, which is closely associated with extracellular matrix (ECM) remodeling and cellular contractility. Key genes within this module were further selected to develop a CAF-related prognostic risk scoring model (riskScore) with robust stability and independent predictive value. In addition, through cell–cell communication analysis combined with spatial transcriptomic data, we revealed the central role of CAFs in the COLLAGEN signaling pathway and their spatial co-localization with immunosuppressive cells, suggesting that CAFs may mediate immune cell exclusion via a dual mechanism involving both physical barriers and functional suppression. Overall, this study systematically delineates the CAF-driven immune exclusion network, proposes CAF functional features with clinical prognostic and therapeutic potential, and provides a new theoretical basis for optimizing immunotherapy strategies.

2 Materials and methods

2.1 Study design

We first conducted single cell analysis in GSE215120 in melanoma. Additionally, High Dimensional Weighted Gene Co-expression Network Analysis (hdWGCNA) was performed to classify gene modules associated with CAFs in the GSE215120. Machine learning was employed to identify significant prognostic genes in gene modules. Receiver Operating Characteristic (ROC) analysis, Kaplan–Meier (KM) survival analysis, and a nomogram were utilized to evaluate the model's performance. Finally, Spatial Transcriptomics was conducted to validate our findings. The complete workflow of our study is illustrated in Fig. 1.

2.2 Data sources

Multiple datasets were obtained from the Gene Expression Omnibus (GEO) database and The Cancer Genome Atlas (TCGA) for this study, including GSE215120, TCGA-SKCM and GSE250636.

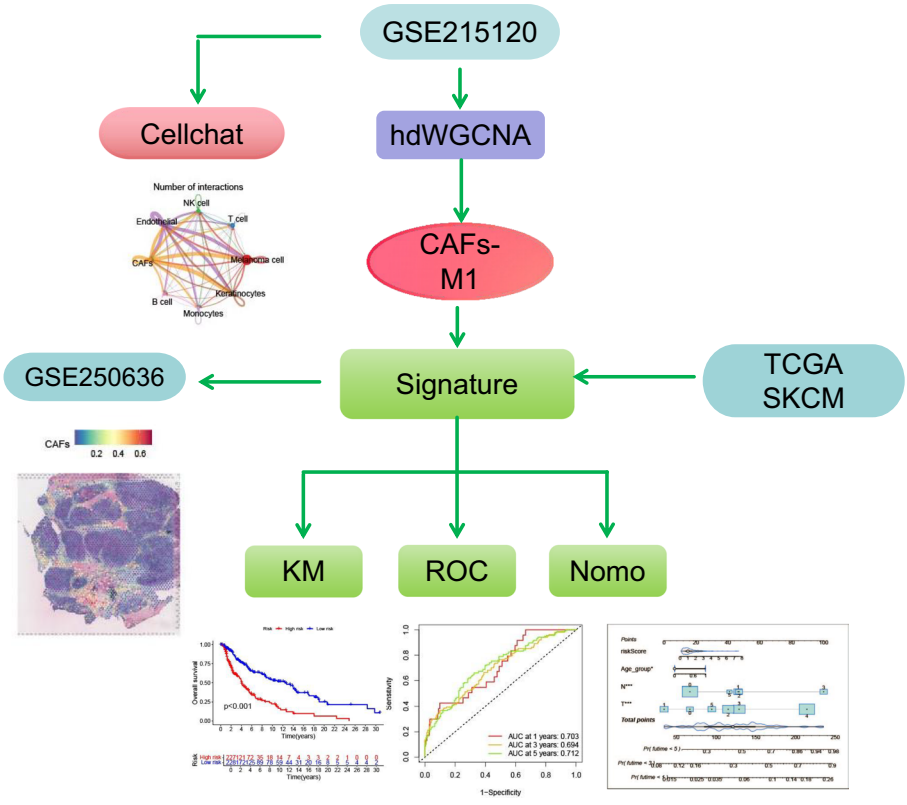

Fig. 1 Flowchart of the analysis. KM-Kaplan–Meier, ROC- Receiver Operating Characteristic, Nomo-Nomogram, Signature—Risk score genes

2.3 Analysis of scRNA -seq datasets

Firstly, we used the Seurat R package to cluster the single-cell dataset GSE215120 and performed basic cell annotation. Cells with a gene count between 300 and 8000, or with a mitochondrial gene ratio of less than 10%, were selected to exclude potential low-quality cells. Harmony was applied to eliminate batch effects among samples, followed by Principal Component Analysis (PCA) for dimensionality reduction, and UMAP for visualization.To identify gene co-expression modules associated with specific biological features, we performed high-dimensional Weighted Gene Co-expression Network Analysis (hdWGCNA). The hdWGCNA pipeline was applied to the single-cell expression matrix after quality control and normalization [13]. The default parameters for hdWGCNA include a gene selection method based on expression in a fraction of cells (0.05), a soft threshold power of 7. Subsequently, CellChat R package was used for intercellular communication analysis to identify actively communicating cells associated with CAFs.

2.4 Establishment of the prognostic model

Univariate Cox regression, least absolute shrinkage and selection operator (LASSO), and multivariate Cox regression analyses were performed to identify independent prognostic factors in the TCGA-SKCM cohort, with $p < 0.05$ considered statistically significant. Finally, nine genes were selected and incorporated into the prognostic model. Equation and calculation of risk score was in Supplemental Table 1.

2.5 Analysis of spatial transcriptomics

To assess background signal and validate the specificity of cell-type deconvolution in spatial transcriptomics data, we applied SpaCET and RCTD R packages to both tissue-covered and blank regions to perform cell-type deconvolution based on reference single-cell RNA-seq data [14, 15]. The goal was to evaluate whether inferred cell-type proportions in the blank areas deviated from expected null distributions. Deconvolution results from the blank regions were compared with those from tissue regions to assess the signal-to-noise ratio and to determine an appropriate confidence threshold for downstream biological interpretation. Spatial feature expression plots were generated utilizing the "SpatialFeaturePlot" function within the "Seurat" R package.

3 Result

3.1 Single-cell transcriptome of patients with melanoma

Through our single-cell analysis, we identified a total of 8 distinct cell types, including Melanoma cell, T cell, NK cell, Endothelial, CAFs, B cell, Monocytes, and Keratinocytes, as shown in Fig. 2A. In our study, single-cell RNA sequencing was performed, yielding a total of 58,418 cells, including 35,422 melanoma cells, 8561 T cells, 7315 NK cells, 2203 endothelial cells, 2695 CAFs, 1295 B cells, 846 monocytes, and 81 keratinocytes. Furthermore, the cellular composition of each sample is illustrated in Fig. 2B. Moreover, UMAP projections of scRNA-seq data further classified these 8 distinct cell types, with representative marker genes, including Melanoma cell(PMEL), T cell(CD3D), NK cell(NKG7), Endothelial(VMF), CAFs(COL1A1), B cell(MS4A1),Monocytes(LYZ),and Keratinocytes(KRT14), as shown in Fig. 2C and 2D. Additionally, we presented a volcano plot to visualize the differentially expressed genes (DEGs) of each cell type, as shown in Fig. 2E. Furthermore, we performed functional analyses on different cell types to illustrate their biological roles, as depicted in Fig. 2F. We have also performed clustering to identify CAF subpopulations, with the corresponding cell types and clusters visualized in the UMAP projections presented in Supplemental Fig. 7A and Supplemental Fig. 7B. ACTA2, CXCL12, and SPP1 represent the markers for myCAF, iCAF, and apCAF, respectively in Supplemental Fig. 7C. As shown in Supplemental Fig. 7D, Supplemental Fig. 7E and Supplemental Fig. 7F, the word cloud, volcano plot, and KEGG enrichment results collectively reveal the distinct biological functions and significance of the three cell subpopulations.

3.2 Identification of gene modules associated with CAFs in melanoma

The hdWGCNA algorithm was employed to identify core genes associated with CAFs. Moreover, hdWGCNA is designed to decipher continuous, co-expression gene programs. A flexible threshold of 7 was selected to divide the genes into 16 functional modules in Fig. 3A and B. The interrelationships among the 16 gene modules were analyzed and are visualized in Fig. 3C. CAFs module has the highest correlation with genes in the CAFs-M1 module in Fig. 3D and 3F. The marker genes characterizing the CAFs-M1 population are presented in Fig. 3E. Gene Ontology (GO) enrichment analysis was performed on 325 CAF-associated genes, and the results are presented in Figs. 3G and 3H. The distribution of genes from each module, projected in the reduced dimensional space, is presented in Supplemental Fig. 1.

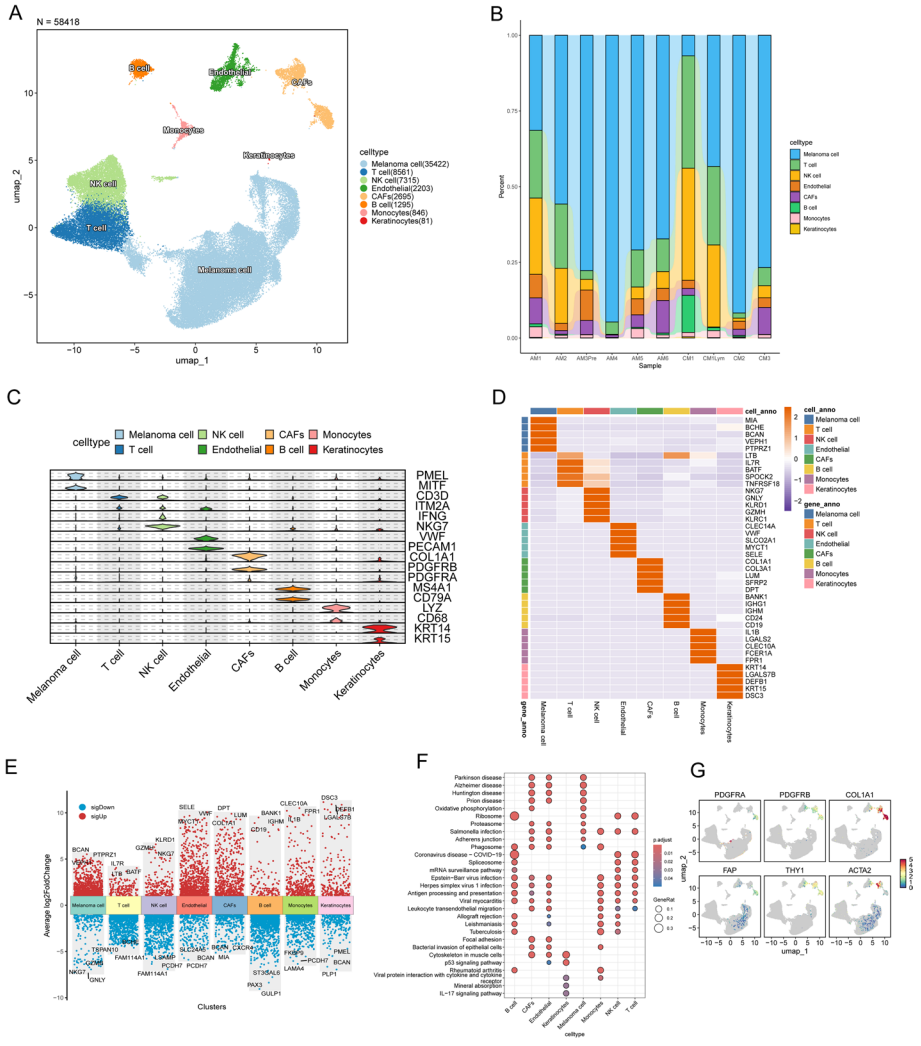

Fig. 2 **A**: UMAP projection of single-cell celltype. **B**: Relative abundance of 10 distinct samples. **C**: Violin plot displaying marker gene expression for the 8 distinct cell types. **D**: Heatmap of gene expression across the 8 distinct cell types. **E**: Volcano plot of differentially expressed genes (DEGs) across the 8 distinct cell types. **F**: Functional annotation of the 8 distinct cell types. **G**: Featureplots of CAF marker genes

3.3 Construction of a melanoma signature prediction model in machine learning

The outcomes of the LASSO regression, including feature selection and model fitting, are presented in Figs. 4A and 4B**.** Based on the integrated analysis of hdWGCNA, LASSO, univariate Cox, and multivariate Cox regression, a total of nine genes were ultimately included in the model in Figs. 4C**.** The survival time and risk index were visualized and are presented in Fig. 4D. The expression patterns of the model genes are visualized by the heatmap in Fig. 4E. The single-cell UMAP projection of the genes included in the model is displayed in Supplemental Fig. 2. Additionally, the prognostic significance of the model features was evaluated using Kaplan–Meier (KM) curves, with results demonstrating statistical significance ($p < 0.05$) and time-dependent ROC curves in Fig. 4F and G. Univariate analysis yielded a riskScore = 1.733 (95% CI: 1.557–1,929, $p < 0.001$), while multivariate analysis showed a riskScore = 1.673 (95% CI: 1.500–1.865, $p < 0.001$), as presented in Fig. 5A and 5B. Notably, our model consistently outperformed individual prognostic indices in predictive capability, as demonstrated in Fig. 5C, 5D, 5E and 5F.

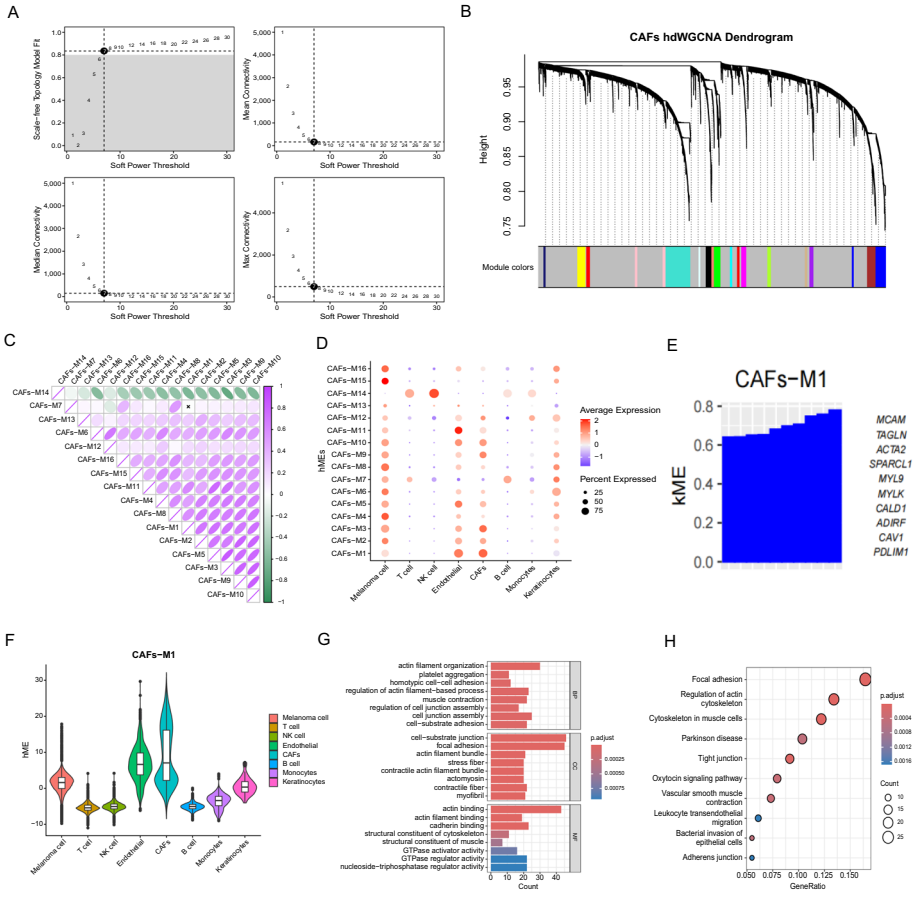

Fig. 3 **A**: Soft threshold selection plot to determine the optimal threshold. **B**: Gene module clustering diagram. **C**: The correlation relationships among the 16 gene modules. **D**, **F**: The importance of each gene module across various cell types. **E**: Signature genes of the CAFs-M1 subtype. **G**, **H**: Functional annotation of the CAFs-M1 module

3.4 The critical role of collagen signaling pathway between CAFs and melanoma cell

To explore which cell types CAFs mainly interact with, we performed CellChat analysis. Meanwhile, CAFs were found to play a pivotal role in cellular communication, as illustrated in Fig. 6A and 6B**.** The critical role of the COLLAGEN signaling pathway in regulating interactions between CAFs and melanoma is demonstrated in Figs. 6C, 6E, and 6F. To comprehensively evaluate the functional significance of each signaling pathway, heatmaps and dot plots were employed for visualization and comparison in Figs. 6D and 6G. Subsequently, collagen signaling pathway associated genes were visualized across different cell types in Fig. 6H.

3.5 Spatial transcriptomics reveals the spatial distribution of cell types in melanoma

To investigate the spatial distribution of cell types, we performed spatial transcriptomic analysis. The deconvolution results obtained using RCTD are shown in Fig. 7A. The projection of the model genes onto the spatial transcriptomic data is shown in Supplemental Fig. 3. To explore the intensity of intercellular communication within the spatial context, we applied MISTy for cell–cell interaction analysis in Fig. 7B**.** The results of spatial deconvolution performed by SpaCET are displayed in Supplemental Fig. 4**.** Based on this deconvolution method, the results of cell–cell interactions are shown in Fig. 7C**.**

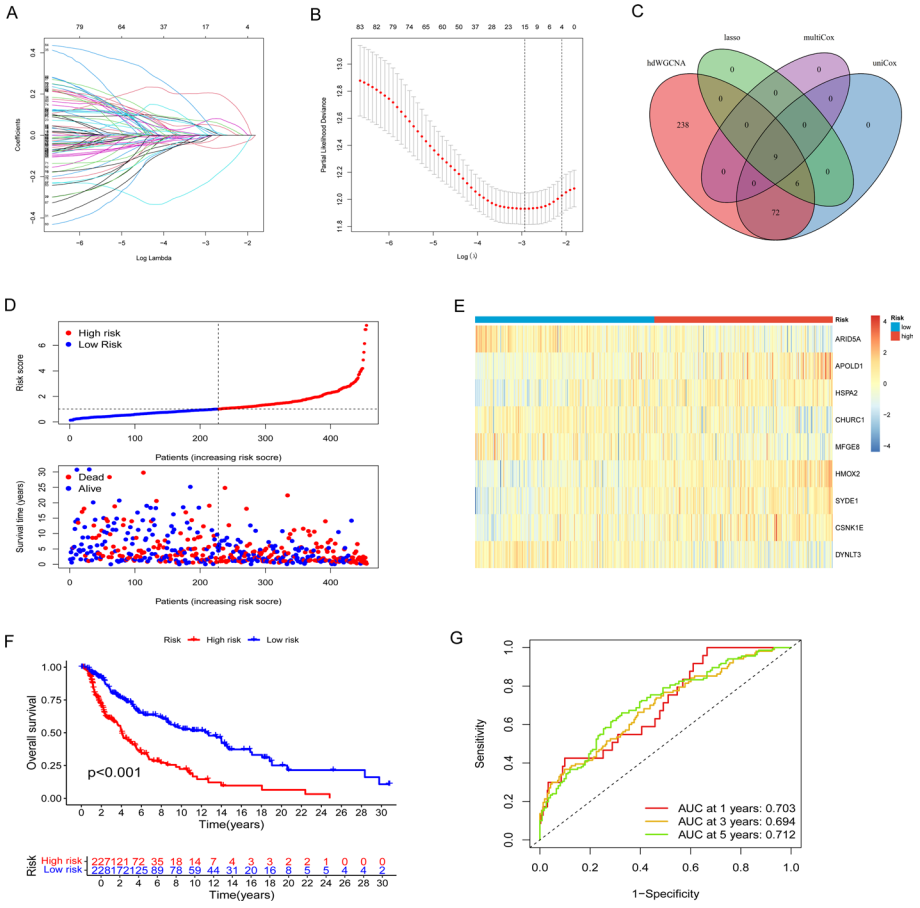

Fig. 4 **A**: LASSO coefficient profiles of the candidate genes. **B**: Ten time cross-validation for tuning parameter selection in the LASSO. **C**: Venn diagram showing the overlap of gene sets identified from different analyses. **D**: Distribution of survival time and risk score for each patient. **E**: Heatmap of the expression profiles of the model genes across low and high group. **F**: Kaplan–Meier survival curves for high- and low-risk groups. **G**: Time-dependent ROC curves for the prognostic model at 1, 3, and 5 years

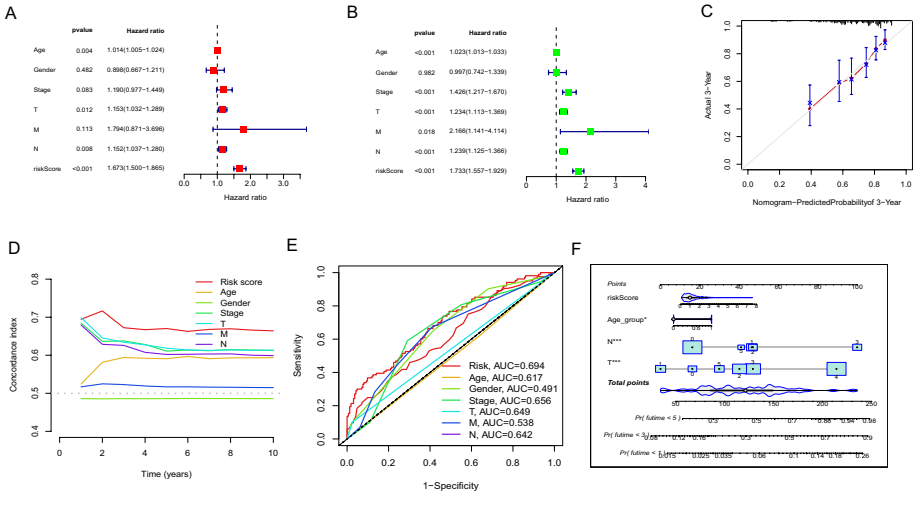

Fig. 5 **A–B**: Multivariate analysis and univariate analysis for clinical indices along with the model risk score. **C**: Nomogram predicting the 3 year overall survival probability. **D**: C-index for clinical indices along with the model risk score. **E**: ROC curves for clinical indices along with the model risk score. **F**: Nomogram integrating model risk score and clinical indices. T represents Tumor size, M represents Metastasis, and N represents Node status

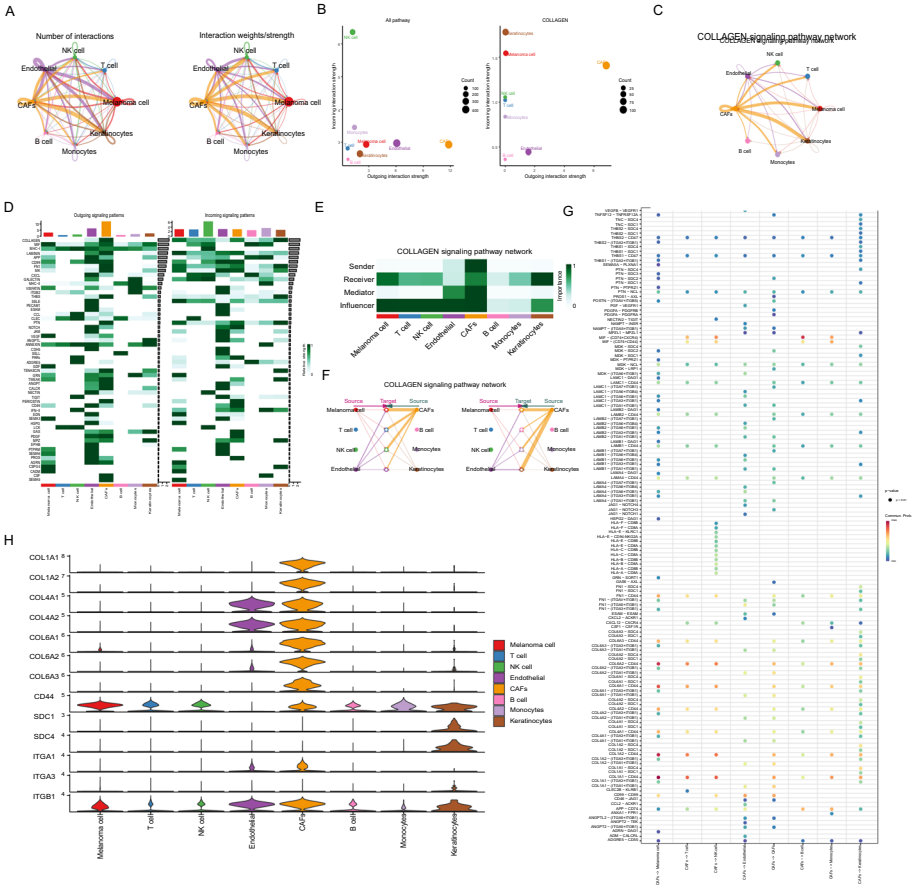

Fig. 6 **A**: Number of interactions and interaction weights among 8 distinct cell types. **B**: Intercellular communication analysis for all pathway and COLLAGEN. **C**, **E** and **F**: COLLAGEN signaling pathway network among 8 distinct cell types. **D**, **G**: Heatmaps and dot plots among 8 distinct cell types

Through SpaCET, we found that CAFs and endothelial cells exhibit similar expression patterns, which may provide a basis for the prognostic value of CAFs.

4 Discussion

In recent years, studies have increasingly revealed the multifaceted roles of CAFs in tumor immune evasion. CAFs not only promote the recruitment and activation of regulatory T cells (Tregs) by secreting immunosuppressive factors such as TGF-β and CXCL12, thereby suppressing effector immune responses, but also construct dense extracellular matrix (ECM) barriers that impede the infiltration of $CD8^+$ T cells into the tumor core, collectively contributing to the formation of an "immune-excluded" microenvironment [16, 17]. Some studies have indicated that the prostaglandin E2 (PGE2) pathway, which is highly expressed by cancer-associated fibroblasts (CAFs), is closely associated with the proliferation of tumor cells. In a neuroblastoma xenograft model, a significant decrease in tumor cell proliferation was observed through immunohistochemical staining following the inhibition of the PGE2 pathway by microsomal prostaglandin E synthase-1 (mPGES-1) inhibitors [18, 19]. However, most previous studies have relied on traditional markers such as FAP and α-SMA for static classification of CAFs, which fails to capture the dynamic transcriptional continuum and functional heterogeneity underlying CAF behavior [6].

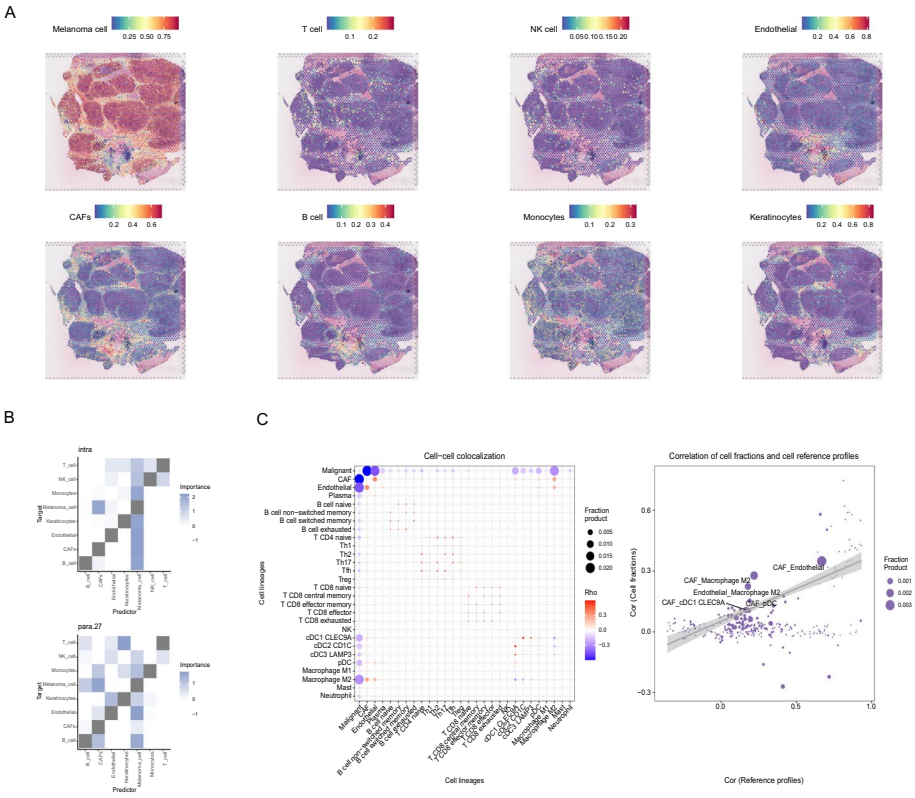

Fig. 7 **A**: Cell-type distribution based on RCTD deconvolution results. **B**: MISTy heatmap result among 8 distinct cell types. **C**: Cell – cell colocalization and Correlation of cell fractions and cell reference profiles among 8 distinct cell types in SpaCET

This study focuses on melanoma, a highly immunogenic but markedly heterogeneous tumor type, and systematically investigates the molecular characteristics of CAFs and their roles in shaping an immune-excluded microenvironment. By integrating single-cell transcriptomic, spatial transcriptomic, and bulk RNA sequencing data, we employed weighted gene co-expression network analysis (WGCNA) to identify functional modules within CAFs. A total of 16 CAF-specific functional modules were identified, among which the CAF-M1 module was significantly enriched in actin cytoskeleton remodeling, extracellular matrix (ECM) organization, and cell adhesion pathways, exhibiting a typical "contractile" CAF phenotype. The CAF-M1–based risk scoring model (riskScore) we constructed accurately reflected stromal activation and immune exclusion status and demonstrated robust prognostic performance across multiple melanoma cohorts. Furthermore, riskScore functioned as an independent risk factor with strong generalizability and clinical stratification value.

Spatial transcriptomics and cell–cell communication analyses further revealed that CAF-M1 cells were highly co-localized with M2 macrophages and endothelial cells, and established dense interaction networks with various immune-related cell populations via the COLLAGEN–integrin signaling axis. A recent study reveals that FAP$^+$CAFs are the predominant stromal cell population associated with adverse clinical outcomes and immunosuppressive phenotypes in breast cancer. Mechanistically, FAP$^+$CAFs secrete high levels of fibronectin 1 (FN1), which interacts with integrin α5β1 on macrophages to activate the FAK-AKT-STAT3 signaling pathway. This interaction drives macrophages toward an immunosuppressive M2-like phenotype, thereby contributing to the

establishment of an immunosuppressive tumor microenvironment.(40,263,422) Genetic deletion of HIF-1α in myeloid cells reduced the expression of fibroblast-activating factors in tumor-associated macrophages (TAMs), thereby decreasing cancer-associated fibroblast (CAF) abundance and suppressing tumor formation [20]. This dual mechanism—comprising structural barrier formation and signaling-mediated immune suppression—represents a CAF-driven immune exclusion architecture that has not been systematically characterized in previous studies focused primarily on soluble factors or single-pathway interactions. Our findings expand the current framework for CAF heterogeneity profiling and highlight the pivotal role of the CAF-M1 subpopulation in constructing "immune-cold" tumors. The proposed riskScore model holds promise as a precision tool for pre-immunotherapy assessment and offers both a theoretical foundation and practical reference for individualized patient stratification and CAF-targeted therapeutic strategies.

Through detailed analysis of the gene composition within the CAF-M1 module, we found that several key molecules not only play central roles in maintaining the structural functions of CAFs but also are crucial in shaping the immune microenvironment and mediating immune cell exclusion. Cytoskeletal regulatory genes such as ACTA2, TAGLN, MYLK, and CALD1 enhance the contractility and tension of CAFs, promoting the formation of dense stromal structures within tumor tissues—physical barriers widely considered to directly impede $CD8^+$ T cell infiltration into the tumor core [21–23]. Meanwhile, extracellular matrix components and crosslinking factors including COL1A1, COL3A1, LOXL2, and FN1 are significantly enriched in the CAF-M1 module, indicating this subpopulation's high activity in collagen deposition, matrix densification, and tissue stiffening, which further reinforces the structural basis of immune exclusion [24, 25]. Specifically, COL1A1 and COL3A1 constitute the core framework of the ECM; LOXL2, a lysyl oxidase, crosslinks collagen fibers to increase matrix stiffness and stability [26]; and FN1 (fibronectin), a key glycoprotein involved in ECM assembly and cell adhesion, acts as a scaffold for collagen fiber organization and structural integrity [27]. The concerted action of these molecules creates a dense and rigid ECM environment that promotes tumor progression and contributes to resistance to therapies, including immune checkpoint inhibitors.

Notably, as shown in Fig. 7, our spatial transcriptomics and cell–cell communication analyses further revealed that CAF-M1 is often enriched at the boundaries between immune and non-immune regions within the tissue microenvironment, exhibiting strong spatial co-localization particularly with M2 macrophages and endothelial cells. This forms a "non-immune cell barrier zone" encircling the tumor core. More importantly, CAF-M1 engages in a high-intensity signaling interaction network centered around the COLLAGEN–integrin axis, through collagen-related ligands such as COL1A1/2, interacting with macrophages, tumor cells, endothelial cells, and dendritic cells. This dual mechanism—comprising both matrix construction and signaling regulation—suggests that CAF-M1 not only acts as a physical barrier limiting T cell infiltration but may also regulate immune cell chemotaxis, localization, and activity through immunosuppressive ligand–receptor axes, thereby cooperatively contributing to the sustained maintenance of immune exclusion.

In the CAF-M1–dominated cell communication network of melanoma, in addition to the central COLLAGEN signaling axis, multiple other signaling pathways

closely associated with immune regulation were found to be highly active. For example, CAF-M1 engages in strong interactions with immune cells through pathways such as THBS1–CD47, SPARC–ITGB1, and PDGFB–PDGFRB, potentially modulating their activation states and spatial distribution. Chemotaxis-related axes like CXCL12–CXCR4 and ANGPTL4–S1PR1 may regulate immune cell homing and migration trajectories, while the TGF-β signaling axis is likely involved in the induction of T cell exhaustion and impairment of antigen presentation [28, 29]. Moreover, several core genes within the CAF-M1 module play pivotal roles in mediating these signaling interactions. For instance, THBS1 and SPARC may enhance the immunosuppressive effects of CAFs on $CD8^+$ T cells and dendritic cells via integrin pathways (e.g., ITGA5/ITGB1) and the TGF-β pathway, potentially promoting T cell exhaustion and diminishing antigen presentation capacity, respectively [30, 31]. PDGFRB and MMP11 participate in ECM remodeling and the release of chemotactic factors (such as CCL2 and CXCL1), thereby regulating the recruitment and M2 polarization of macrophages and neutrophils to shape an immunosuppressive milieu [32, 33]. CAF-M1 is also enriched in immunomodulatory genes such as VCAN, POSTN, LAMA4, and TNC, which may influence immune cell adhesion, migration, and inflammatory signaling thresholds through interactions with surface receptors like CD44, syndecans, and integrins; notably, POSTN has been associated with immunotherapy resistance in various cancers [34]. Although FAP, PDPN, and MFAP5 were not included in the final risk model, their high expression within the CAF-M1 subpopulation suggests they may represent activation features of immunoregulatory CAFs beyond structural roles. Taken together, CAF-M1 in melanoma not only establishes stable interactions with diverse immune cells via the COLLAGEN axis but also, through its spatial enrichment and multifaceted signaling capabilities, constructs an integrated "physical barrier + signaling suppression" immune exclusion system, serving as a central hub for CAF-driven immunologically cold tumor environments.

In addition, we validated the spatial expression patterns of the key genes included in the risk scoring model and found that molecules such as MFGE8, HMOX2, HSPA2, SYDE1, APOLD1, and ARID5A exhibited clear expression bias in CAF-enriched regions, further supporting their consistency with immune microenvironment remodeling and CAF-M1 localization. Among them, MFGE8 has been shown to contribute to immune tolerance in various tumors by promoting M2 macrophage polarization and suppressing T cell activity [35, 36]; HMOX2 is closely associated with oxidative stress and anti-inflammatory responses and may mediate signaling interactions between CAFs and macrophages [37]; HSPA2 and ARID5A may help maintain CAF activity or promote immune evasion by modulating stress responses and transcriptional regulation [38, 39]. Other scoring genes such as CHURC1, CSNK1E, and DYNLT3, though their roles in tumor immunity have not been fully elucidated, showed spatial co-expression patterns aligned with CAF localization, suggesting their potential involvement in CAF state transitions or immune regulation, warranting further investigation. These findings not only enhance the spatial interpretability of the risk model but also indicate that certain risk score genes may possess intrinsic immunomodulatory functions and hold promise as auxiliary targets for future therapeutic interventions.

5 Conclusions

This study identifies a contractile CAF-M1 subpopulation in melanoma that contributes to immune exclusion by remodeling the extracellular matrix and engaging in immunosuppressive signaling. CAF-M1 shows strong spatial co-localization with M2 macrophages and endothelial cells, forming a physical and functional barrier to immune infiltration. A risk score model based on CAF-M1–related genes demonstrated strong prognostic value and may aid in identifying immune-cold tumors. These findings highlight CAF-M1 as a potential target to improve immunotherapy outcomes in melanoma.

6 Limitation

Although this study systematically elucidated the multifaceted mechanisms by which CAF-M1 contributes to tumor immune exclusion and proposed a novel structure–function framework by integrating spatial transcriptomics and cell–cell communication data, several limitations remain to be addressed. First, the identification and functional inference of the CAF-M1 module were primarily based on transcriptomic data from public databases. While cross-validation across multiple independent melanoma cohorts supports the robustness of our findings, direct evidence at the protein level or from functional experiments using clinical samples is still lacking, and the clinical applicability and biological causality of the model require further empirical validation. Additionally, CAFs exhibit tissue-specific characteristics across different cancer types, and their activation states, immunoregulatory capacities, and functional modalities may be influenced by tumor type and evolutionary stage. Thus, the conservation and generalizability of the CAF-M1 module in other solid tumors remain to be fully evaluated. Future studies incorporating CAF lineage tracing, functional perturbation experiments in animal models, and combined immunotherapy interventions could provide systematic validation of the causal role of CAF-M1 in reshaping the tumor immune microenvironment and modulating therapeutic responses, thereby advancing its translational potential in both mechanistic research and clinical application.

Supplementary Information

The online version contains supplementary material available at https://doi.org/10.1007/s12672-025-03868-3.

Supplementary material 1. Figure S1: Gene module identification and correlation with cell types.

Supplementary material 2. Figure S2: Single-cell level visualization of model gene expression.

Supplementary material 3. Figure S3. Spatial expression patterns of model genes in the spatial transcriptomic dataset,

Supplementary material 4. Figure S4. Cell-type composition inferred from spatial transcriptomics using SpaCET.

Supplementary material 5. Figure S5. Umap it with batch correction.

Supplementary material 6 Figure S6: Umap it without batch correction.

Supplementary material 7 Figure S7. A: UMAP projection of cluster in CAFs. B: Cell type identification of CAF subpopulations. C: Dotplot for CAF subpopulations markers. D: Word cloud of CAF subpopulations. E: Volcano plot of CAF subpopulations. F: KEGG enrichment results of CAF subpopulations.

Supplementary material 8. Table S1： Results of Multivariate Cox Regression Analysis.

Acknowledgements
Not applicable.

Author contributions
LZ and WS, as the total corresponding Authors, guided the design of the entire experiment and the writing of the paper. SH, YZ, AH, and YZ have been involved in data collection and data analysis, and they contributed equally. YL, YR

and ZL have been involved in data interpretation, drafting the manuscript and revising it critically and have given final approval of the version to be published.

Funding
This work was supported by the Youth Development Project Fund of the First Affiliated Hospital of Naval Military Medical University (Grant No. 2021JCQN09), the Special Fund for Basic Research of Naval Military Medical University (Grant No. 2022QN061), and the Clinical Research Plan of Shanghai Hospital Development Center (SHDC) (Grant No. SHDC22022302).

Data availability
The datasets analyzed during the current study are publicly available. The gene expression profiles GSE215120 and GSE250636 can be accessed from the Gene Expression Omnibus (GEO) database (https://www.ncbi.nlm.nih.gov/geo/). The TCGA-SKCM dataset is available from The Cancer Genome Atlas (TCGA) via the Genomic Data Commons (GDC) portal (https://portal.gdc.cancer.gov/). All data used in this study are open access and do not require special permissions for use.

Declarations

Ethics approval and consent to participate
Not applicable.

Consent for publication
Not applicable.

Competing interests
The authors declare no competing interests.

Author details
[1]Department of Dermatology, First Affiliated Hospital of Naval Military Medical University, Shanghai, China
[2]Clinical School of Medicine, Anhui Medical University, No. 1166, West Wangjiang Road, Shushan District, Hefei 230601, China
[3]Department of Chemical and Biological Engineering, The Hong Kong University of Science and Technology, Hong Kong SAR, China
[4]College of Anesthesia, Wannan Medical College, No. 22 Wenchang West Road, Yijiang District, Wuhu 241002, Anhui, China
[5]First Clinical Medical College (First Affiliated Hospital), Anhui Medical University, 81 Meishan Road, Hefei 230032, China
[6]The First Affiliated Hospital of Anhui Medical University, No. 218, Jixi Road, Shushan District, Hefei 230032, China

Received: 29 June 2025 / Accepted: 13 October 2025
Published online: 14 November 2025

References

1. Long GV, Swetter SM, Menzies AM, et al. Cutaneous melanoma. Lancet. 2023;402(10400):485–502. https://doi.org/10.1016/s0140-6736(23)00821-8.
2. Arnold M, Singh D, Laversanne M, et al. Global burden of cutaneous melanoma in 2020 and projections to 2040. JAMA Dermatol. 2022;158(5):495–503. https://doi.org/10.1001/jamadermatol.2022.0160.
3. Patel M, Eckburg A, Gantiwala S, et al. Resistance to molecularly targeted therapies in melanoma. Cancers. 2021. https://doi.org/10.3390/cancers13051115.
4. Noringriis IM, Donia M, Madsen K, et al. Long-term clinical outcome of patients with metastatic melanoma and initial stable disease during anti-PD-1 checkpoint inhibitor immunotherapy with pembrolizumab. Br J Cancer. 2025. https://doi.org/10.1038/s41416-025-03048-8.
5. Yin T, Wang G, Wang L, et al. Breaking NGF-TrkA immunosuppression in melanoma sensitizes immunotherapy for durable memory T cell protection. Nat Immunol. 2024;25(2):268–81. https://doi.org/10.1038/s41590-023-01723-7.
6. Mu G, Zhang W, Huang J, et al. Research status of tumor-associated fibroblasts regulating immune cells. Zhongguo Fei Ai Za Zhi. 2022;25(3):207–13. https://doi.org/10.3779/j.issn.1009-3419.2022.101.04.
7. Feng B, Wu J, Shen B, et al. Cancer-associated fibroblasts and resistance to anticancer therapies: status, mechanisms, and countermeasures. Cancer Cell Int. 2022;22(1):166. https://doi.org/10.1186/s12935-022-02599-7.
8. Forsthuber A, Aschenbrenner B, Korosec A, et al. Cancer-associated fibroblast subtypes modulate the tumor-immune microenvironment and are associated with skin cancer malignancy. Nat Commun. 2024;15(1):9678. https://doi.org/10.1038/s41467-024-53908-9.
9. Kanzaki R, Pietras K. Heterogeneity of cancer-associated fibroblasts: opportunities for precision medicine. Cancer Sci. 2020;111(8):2708–17. https://doi.org/10.1111/cas.14537.
10. Liu Y, Sinjab A, Min J, et al. Conserved spatial subtypes and cellular neighborhoods of cancer-associated fibroblasts revealed by single-cell spatial multi-omics. Cancer Cell. 2025;43(5):905-924.e6. https://doi.org/10.1016/j.ccell.2025.03.004.
11. Yang KL, Sun Z, Bai CM, et al. application of single-cell RNA sequencing in research on tumor immune microenvironment. Zhongguo Yi Xue Ke Xue Yuan Xue Bao. 2020;42(1):117–23. https://doi.org/10.3881/j.issn.1000-503X.11194.
12. Ma C, Yang C, Peng A, et al. Pan-cancer spatially resolved single-cell analysis reveals the crosstalk between cancer-associated fibroblasts and tumor microenvironment. Mol Cancer. 2023;22(1):170. https://doi.org/10.1186/s12943-023-01876-x.
13. Morabito S, Reese F, Rahimzadeh N, et al. Hdwgcna identifies co-expression networks in high-dimensional transcriptomics data. Cell Rep Methods. 2023;3(6):100498. https://doi.org/10.1016/j.crmeth.2023.100498.

14. Ru B, Huang J, Zhang Y, et al. Estimation of cell lineages in tumors from spatial transcriptomics data. Nat Commun. 2023;14(1):568. https://doi.org/10.1038/s41467-023-36062-6.
15. Cable DM, Murray E, Zou LS, et al. Robust decomposition of cell type mixtures in spatial transcriptomics. Nat Biotechnol. 2022;40(4):517–26. https://doi.org/10.1038/s41587-021-00830-w.
16. Li G, He J, Wang Q. Progress on cancer associated fibroblasts in tumor immunoregulation. Zhejiang Da Xue Xue Bao Yi Xue Ban. 2018;47(5):558–63. https://doi.org/10.3785/j.issn.1008-9292.2018.10.17.
17. de Visser KE, Joyce JA. The evolving tumor microenvironment: from cancer initiation to metastatic outgrowth. Cancer Cell. 2023;41(3):374–403. https://doi.org/10.1016/j.ccell.2023.02.016.
18. Kock A, Larsson K, Bergqvist F, et al. Inhibition of microsomal prostaglandin E synthase-1 in cancer-associated fibroblasts suppresses neuroblastoma tumor growth. EBioMedicine. 2018;32:84–92. https://doi.org/10.1016/j.ebiom.2018.05.008.
19. Elwakeel E, Brüggemann M, Wagih J, et al. Disruption of prostaglandin E2 signaling in cancer-associated fibroblasts limits mammary carcinoma growth but promotes metastasis. Cancer Res. 2022;82(7):1380–95. https://doi.org/10.1158/0008-5472.Can-21-2116.
20. Rohwer N, Jumpertz S, Erdem M, et al. Non-canonical HIF-1 stabilization contributes to intestinal tumorigenesis. Oncogene. 2019;38(28):5670–85. https://doi.org/10.1038/s41388-019-0816-4.
21. Jin H, Liu B, Guo X, et al. MYLK and CALD1 as molecular targets in bladder cancer. Medicine. 2023;102(47):e36302. https://doi.org/10.1097/md.0000000000036302.
22. Naito K, Sangai T, Yamashita K. Caf-associated genes in breast cancer for novel therapeutic strategies. Biomedicines. 2024. https://doi.org/10.3390/biomedicines12091964.
23. Shah R, Johnson KA, Lippert AEL, et al. Cancer-associated fibroblast proteins as potential targets against colorectal cancers. Cancers. 2024. https://doi.org/10.3390/cancers16183158.
24. Zhang M, Zhang B. Extracellular matrix stiffness: mechanisms in tumor progression and therapeutic potential in cancer. Exp Hematol Oncol. 2025;14(1):54. https://doi.org/10.1186/s40164-025-00647-2.
25. Popovic A, Tartare-Deckert S. Role of extracellular matrix architecture and signaling in melanoma therapeutic resistance. Front Oncol. 2022;12:924553. https://doi.org/10.3389/fonc.2022.924553.
26. Cano A, Eraso P, Mazón MJ, et al. LOXL2 in cancer: a two-decade perspective. Int J Mol Sci. 2023. https://doi.org/10.3390/ijms241814405.
27. Spada S, Tocci A, Di Modugno F, et al. Fibronectin as a multiregulatory molecule crucial in tumor matrisome: from structural and functional features to clinical practice in oncology. J Exp Clin Cancer Res. 2021;40(1):102. https://doi.org/10.1186/s13046-021-01908-8.
28. Yang Y, Li J, Lei W, et al. CXCL12-CXCR4/CXCR7 axis in cancer: from mechanisms to clinical applications. Int J Biol Sci. 2023;19(11):3341–59. https://doi.org/10.7150/ijbs.82317.
29. Zhang C, Fei Y, Wang H, et al. CAfs orchestrates tumor immune microenvironment-a new target in cancer therapy? Front Pharmacol. 2023;14:1113378. https://doi.org/10.3389/fphar.2023.1113378.
30. Li Z, Calzada MJ, Sipes JM, et al. Interactions of thrombospondins with alpha4beta1 integrin and CD47 differentially modulate T cell behavior. J Cell Biol. 2002;157(3):509–19. https://doi.org/10.1083/jcb.200109098.
31. Alcaraz LB, Mallavialle A, Mollevi C, et al. Sparc in cancer-associated fibroblasts is an independent poor prognostic factor in non-metastatic triple-negative breast cancer and exhibits pro-tumor activity. Int J Cancer. 2023;152(6):1243–58. https://doi.org/10.1002/ijc.34345.
32. Zhang X, Huang S, Guo J, et al. Insights into the distinct roles of MMP-11 in tumor biology and future therapeutics (Review). Int J Oncol. 2016;48(5):1783–93. https://doi.org/10.3892/ijo.2016.3400.
33. Fang Z, Xu X, Tao L, et al. MMP11 as a prognostic biomarker correlated with immune infiltrates in pancreatic adenocarcinoma. J Gastrointest Oncol. 2024;15(3):1224–44. https://doi.org/10.21037/jgo-24-425.
34. Wei T, Wang K, Liu S, et al. Periostin deficiency reduces PD-1(+) tumor-associated macrophage infiltration and enhances anti-PD-1 efficacy in colorectal cancer. Cell Rep. 2023;42(2):112090. https://doi.org/10.1016/j.celrep.2023.112090.
35. Ma Z, Sun Y, Yu Y, et al. Extracellular vesicles containing MFGE8 from colorectal cancer facilitate macrophage efferocytosis. Cell Commun Signal. 2024;22(1):295. https://doi.org/10.1186/s12964-024-01669-9.
36. Mizote Y, Inoue T, Akazawa T, et al. Potent CTLs can be induced against tumor cells in an environment of lower levels of systemic MFG-E8. Cancer Sci. 2024;115(4):1114–28. https://doi.org/10.1111/cas.16099.
37. Chen S, Wang X, Nisar MF, et al. Heme oxygenases: cellular multifunctional and protective molecules against UV-induced oxidative stress. Oxid Med Cell Longev. 2019;2019:5416728. https://doi.org/10.1155/2019/5416728.
38. Zhai LL, Qiao PP, Sun YS, et al. Tumorigenic and immunological roles of heat shock protein A2 in pancreatic cancer: a bioinformatics analysis. Rev Assoc Med Bras. 2022;68(4):470–5. https://doi.org/10.1590/1806-9282.20210495.
39. Nyati KK, Kishimoto T. Recent advances in the role of Arid5a in immune diseases and cancer. Front Immunol. 2021;12:827611. https://doi.org/10.3389/fimmu.2021.827611.

Publisher's Note